Modal Analysis of Different Stator Configurations to Mitigate Electromagnetically Excited Audible Noise and Vibrations of Switched Reluctance Motors

Selma Čorović, Rok Benedetič, and Damijan Miljavec

Department of Mechatronics, Laboratory for Electrical Machines, Faculty of Electrical Engineering
University of Ljubljana, SI1000 Ljubljana, Slovenia
selma.corovic@fe.uni-lj.si, rok.benedetic@gmail.com, damijan.miljavec@fe.uni-lj.si

Abstract ─ The primary objective of this paper was to investigate different stator configurations of switched reluctance motors (SRM) in order to mitigate electromagnetically exited audible noise and vibration. We analyzed natural frequencies of different SRM stator configurations by virtue of modal analysis theory. The three-dimensional numerical modeling of SRM stator geometry was performed by using finite element method. Based on the output results, we propose the solutions on how to select an appropriate stator configuration in order to increase its natural frequencies beyond the resonant operational frequency, and thus, to mitigate the resulting audible noise and vibration. The numerical and analytical results are successfully compared to the published data.

Index Terms ─ Electromagnetic force, finite element analysis, modal analysis, natural frequencies, noise and vibration, switched reluctance machines.

I. INTRODUCTION

A quest for energy efficiency, reliability and cost effectiveness has fostered research and development of switched reluctance motors (SRM) due to the fact that they are comparable or more advantageous over their counterparts [1,2]. Numerous studies demonstrated that the SRM may be competitive electric drive system candidate in different automotive and aerospace applications where high-performance and variable-speed is required [1-5]. In addition, the SRM and the SRM drive systems are receiving considerable attention from academia and industry [6-8]. However, among the major drawbacks that prevent the SRM from being more prominent in many industrial and other applications are acoustic noise and vibrations.

Theoretical analysis predicted and experimental measurements of airborne audible acoustic noise confirmed that dominant component of the SRM acoustic noise and vibration signal is emitted from the machine's stator [9]. It has been found that pronounced acoustic noise occurs when the frequencies of exiting stator radial magnetic forces acting on itself coincide with its natural frequencies. In particular, the level of acoustic noise and vibration strongly depends on the geometry design and material properties of the stator configuration of switched reluctance motors. Therefore, the stator configuration need to be carefully planned and designed within the pre-construction stage of the SRM machine. It has been demonstrated that the acoustic noise and vibrations can be successfully predicted with analytical and numerical mathematical models of the SRM, which were validated with experimental measurements [12-15]. For example, the issue of acoustic noise production have been addressed by varying the combination of stator–rotor poles [10]. The influence of windings and end-bells has also been studied on a commercial SRM configuration with 8/6 stator vs. rotor pole ratio [9]. However, although a large body of literature already exists on the analysis of acoustic noise and vibration of the SRM, an optimum SRM configuration is still a subject of scientific investigation [2,9-14].

The primary objective of this study is to mitigate the electromagnetically exited audible noise and vibration of SRM by altering the natural frequencies of different 3-phase SRM configurations. This study is focused on the natural frequencies for the most critical modal shapes of the small size SRM stator configurations (i.e., up to few kW [12]) by virtue of modal analysis theory. First, the natural frequencies of 3-phase SRM stator SRM configurations with different ratios between stator vs. rotor pole number are numerically analyzed based on 3D finite element modeling. Second, the impact of the SRM stator geometry modifications on its natural frequencies was studied by increasing the numbers of stator poles, by changing the thickness of the stator yoke and by adding the spacers and the end-bells to the analyzed stator geometry. The influence of the stator poles geometry modification on the natural frequencies of the resulting stator geometry was also investigated and new stator geometries are proposed. Finally, the numerical results

Submitted On: May 10, 2017
Accepted On: October 17, 2017

of 3D simulations were compared to the analytical calculations based on Jordan's law. Based on the obtained results the solutions are proposed on how to design an appropriate stator geometry in order to increase its natural frequencies beyond the resonant vibration frequency, and consequently to avoid or mitigate the undesirable acoustic noise.

II. THEORETICAL CONSIDERATION

In our present study we focused on the magnetically excited vibration and acoustic noise of small size (i.e., up to few kW [12]) 3-phase switched reluctance motors by means of modal analysis theory. We investigated the impact of different SRM stator geometry modifications on their natural frequencies and the corresponding modal shapes that are responsible for the majority of vibration and acoustic noise. The stators of SRMs with three different ratios between the number of stator poles N_s vs. number of rotor poles are investigated: N_s/N_r = 6/4, 8/6 and 12/8. (Note: The number of the SRM stator poles is equal to the number of the SRM stator teeth).

The maximum noise of the switched reluctance motors is produced when the harmonics of the excitation frequencies of the magnetic radial force $f_{exc}(n)$ coincide with the natural frequencies of the SRM stator. The excitation frequencies $f_{exc}(n)$ in Hz for harmonic numbers n can be calculated according to Equation (1) [12]:

$$f_{exc}(n) = n \cdot f_p = \frac{n \cdot N_{rp} \cdot \omega_m}{60}, \quad (1)$$

where n is harmonic number (n = 1, 3, 5,….), f_p is the fundamental frequency of the phase current in Hz, N_{rp} is the number of the machine rotor poles and the ω_m is the rotational speed of the machine in rotations per minute.

The most critical modes of vibration of small size machines [12] are the first several modal shapes m (typically m = 0, m = 2, m = 4), while for the medium and large size machines also higher vibrational modal shapes (m > 4) may become also important. The contribution of the modal shapes to the acoustic noise and vibration depend on the stator/rotor configuration of the SRM. Specifically, for the 3-phase SRM with the ratio 6/4 and 8/6 the second-order cylindrical mode, also termed in this case as fundamental mode m = 2 is predominant due to the fact that two opposite stator poles are excited simultaneously. Thus, the radial force acts on the stator between these two poles and further on mechanically ovalises the circumference of the stator's yoke. The 3-phase SRM with N_s/N_r ratio 12/8 the fourth-order mode m = 4 causing double oval deformation (i.e., double ovalisation) on the stator's circumference, due to the fact that four opposite stator poles are excited simultaneously. In this case, m = 4 is responsible for the majority of the emitted acoustic noise and vibration. In this study the most critical modal shapes and the corresponding natural frequencies for 6/4, 8/6 and 12/8 SRM configurations are calculated and compared by virtue of modal analysis.

The determined natural frequencies and mode shapes are solutions of an eigenvalue problem [14, 18] described by a general system of equations of motion, which assumes free vibration and ignores the dumping, Equation (2):

$$\left\{[H] - (\omega)^2[M]\right\} \cdot \{X\} = \{0\}, \quad (2)$$

where [H] and [M] are stiffness matrix and the mass matrix, respectively. The square roots of the eigenvalues are the natural frequencies ω (in radians/sec) of the SRM stator structure. The natural frequencies f in cycles/sec are than calculated as $f=\omega/2\pi$. The eigenvectors {X} represent the mode shapes – the shape assumed by the SRM stator structure when vibrating at frequency f.

The modal analysis of 3D SRM stator structures was performed by numerically solving the Eq. (2) using a commercial finite element based software package Autodesk Inventor Professional 2016 and Matlab R2013a. All numerical simulations were run on a computer platform with 2.7 GHz of CPU speed and 3GB of RAM. The accuracy of the numerical results was controlled by the selection of number of finite elements within the model. The final density of finite element mesh was created by increasing the number of elements until the results of the calculated natural frequencies changed less than 0.5%, and thus the numerical error was negligible. However, it should be noted that the models with high finite element number (high quality of finite element mesh) require significant computational time and computer resources.

Within the final part of the study the natural frequencies of the studied baseline SRM stator geometries were also analytically calculated by employing Jordan's law [14,17] in order to find out wheatear it can be used as a more rapid but approximate solution for calculation of natural frequencies of SRM. The analytical results were then compared to the numerically calculated natural frequencies of the SRM stators in 3D (the geometry data are taken from Table 1 with M270-35A material properties). According to the Jordan's law [14,17] the natural frequency for zero modal shape (m = 0) of the stator can be calculated with Equation (3) [14,17]:

$$f_0 = \frac{1}{2 \cdot \pi} \cdot \sqrt{\frac{E}{\rho \cdot R_c^{\,2} \cdot \Delta_m}}, \quad (3)$$

where E is Young's modulus of the stator core material, ρ is the density of the material composing the stator core, R_c is the mean stator yoke radius, and the Δ_m is the corrective factor [14] that accounts for the effect of the stator poles' mass on the stator natural frequencies. The corrective factor Δ_m can be calculated by Equation (4) [14]:

$$\Delta_m = \frac{m_{sy} + N_s \cdot m_{sp}}{m_{sy}}, \quad (4)$$

where the m_{sy} and m_{sp} stand for the stator yoke mass and the stator pole mass, respectively, whereas the N_s is the number of the stator poles.

According to the Jordan's law [14,17], the natural frequencies for modal shapes $m \geq 2$ are expressed with Equation (5):

$$f_m = \frac{f_0 \cdot w_{sy} \cdot m \cdot \left(m^2 - 1\right)}{2 \cdot \sqrt{3} \cdot R_c \cdot \sqrt{m^2 + 1}}, \quad (5)$$

where f_0 is natural frequency for zero modal shape, w_{sy} is the thickness of the stator yoke, m is the number of the modal shape ($m \geq 2$), and R_c is the mean stator radius without considering the stator poles. The Equations (3) and (5) are derived for 2D structures that represent an approximation of the electrical machine stator with a ring (the stator teeth (i.e., poles) are taken into account by introducing the corrective factor Δ_m (Equation (4)).

III. RESULTS AND DISSCUSION

A. Verification of 3D numerical modeling

Within the first part of the study a preliminary 3D model numerical analysis was done based on the on the reference SRM configuration geometry and its material properties taken from the literature [9,15]. The stator configuration (the SRM with N_s/N_r = 8/6 and the ribbed frame (i.e., stator housing)) of the reference SRM model [9] is based on the modal analysis theory and on experimental validation performed using a shaker-accelerometer system. In order to verify the accuracy of our 3D numerical results, we compared the results of our numerical simulations to the results from the reference study [9]. The 3D model of the SRM stator (N_s = 8) with the ribbed frame geometry used as a reference model for numerical results verification (the model geometry was built according to the dimensions of the model developed in [9]) is shown in Fig. 1 (a). The dimensions are given in millimeters. The 2D view in the central XY cross section of the SRM stator only is shown in Fig. 1 (b). The geometrical parameters in the Fig. 1 (b), the stator yoke thickness w_{sy}, the height of the stator pole h_p (i.e., the stator tooth), the width of the stator pole w_{sp}, the pole arc of stator $ß$, stator outer radius R_{so}, the yoke inner radius R_{sy}, the stator bore radius R_{si} and the length of stator L. According to [9], the values of the geometrical parameters are w_{sy} = 11.4 mm, h_p = 30 mm, w_{sp} = 16.9 mm, $ß$ = 20.2°, R_{so} = 89.8 mm, R_{sy} = 78.4 mm, R_{si} = 48.18 mm, and L = 151 mm. According to [9], the stator was modelled as a ferromagnetic material with the Young's elasticity modulus $E = 2.07*10^{11}$ N/m^2, while the material for the stator frame is cast iron with $E = 1.65*10^{11}$ N/m^2. The mass density of both materials is 7800 kg/m^3.

The calculated natural frequencies for m = 2 and m = 4 obtained in this study were 1331 Hz and 4237 Hz, respectively (as shown in Figs. 2 (a) and 2 (b)). These two frequencies differed from the calculated and measured natural frequencies in [9] by 1.3% and 2.8% for the modal shape 2 and 4, respectively. Thus, a good agreement was obtained between our results and the results previously obtained from [9]. This small difference can be attributed to the difference in geometry of the modeled geometry dimensions that were not available to us from [9]. Namely, the geometry of ribs at the bottom part of the stator frame (present in [9]) was omitted in the model developed in this study. Based on this comparison the preliminary numerical models built in this study were verified. Based on compared results we concluded that the preliminary mode can be successfully used and extended for further analysis performed in this study.

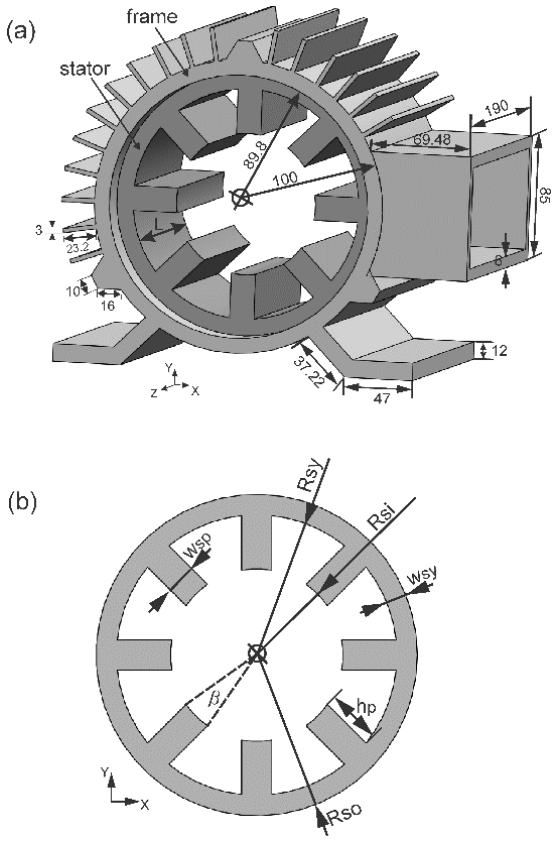

Fig. 1. (a) The 3D model of the SRM stator (N_s = 8) with the ribbed frame geometry used as a reference model for numerical results verification (the model geometry was built according to the dimensions of the model developed in [9]; the dimensions are given in millimeters), and (b) the 2D view in XY cross section of the SRM model with the geometrical parameters.

The numerical results are shown in Fig. 2. The results (i.e., the deflection profiles at the calculated natural frequencies) are displayed in central XY cross-section plane of the 3D finite element models. The grayscale color bar shows relative movement/displacement profile from the minimum (light gray) to maximum (black) value as a result of numerical modal analysis performed

in Autodesk Inventor software we used in our study. The white color in figures represents the stator area where no movement/displacement occurs. The color chart shows relative movement/displacement values based on which the modal shapes are formed. Therefore, the units are not applicable (they have no actual physical value), since the mode shapes values are relative. (Note: This is also valid for the results shown in the Fig. 6 and Fig. 8.)

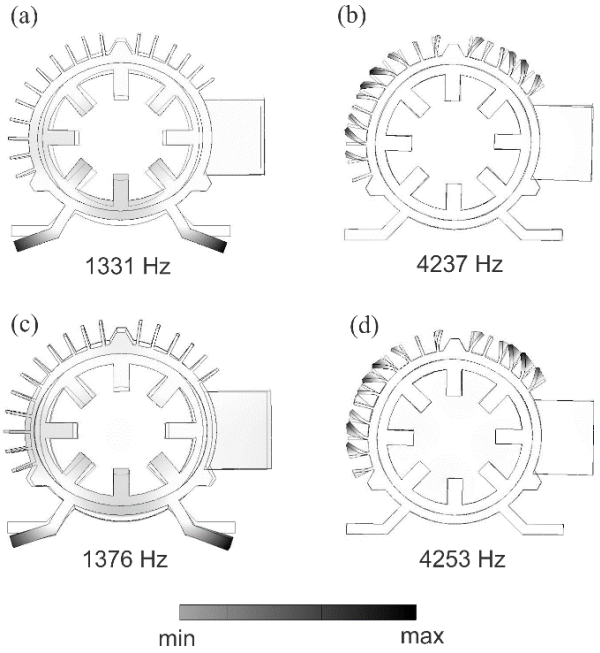

Fig. 2. The calculated deflection profiles and the corresponding frequencies of SRM stators with ribbed frame without end-bells: (a) 1331 Hz and (b) 4237 Hz; and with end-bells: (c) 1376 Hz and (d) 4523 Hz.

The second modal shape (f = 1331 Hz) of the modeled assembly of the SRM stator with ribbed frame is shown in Fig. 2 (a). From the Fig. 2 (a) it can be seen that at lower natural frequency the stator deforms according to the second modal shape, while the stator frame remains still. It is interesting to note that at higher natural frequencies (f = 4237 Hz) the stator remains still while the mechanical vibration and deformation of the stator frame ribs considerably increases, as shown in Fig. 2 (b). In addition, in order to increase the stiffness of the stator geometry the end-bell geometry (illustrated Fig. 5 (b) was also added to the baseline stator geometry and the natural frequencies of the whole assembly were calculated. The calculated and visualized results for the stator assembly with one end-bell are displayed in Figs. 2 (c) and 2 (d). The calculated numerical results shown in Figs. 2 (c) and 2 (d) indicate that if the end-bells are added to the analyzed assembly the vibration of the whole assembly is somewhat constrained, resulting in increase of the natural frequency as compared to the stator assembly without the end-bell. Due to the presence of end-bell the SRM assembly is expected to emit the vibration of higher frequencies compared to the stator assembly without the end-bell. Interestingly, at higher frequencies the ribs of the stator frame starts to vibrate, and thus the mechanical noise and vibration is emitted predominantly due to the frame.

B. Influence of SRM stator geometry modification on its natural frequencies

The SRM stator geometries (with N_s = 6, 8 and 12) given in Fig. 3 served as reference/baseline models for all further geometry modifications and corresponding natural frequency calculations.

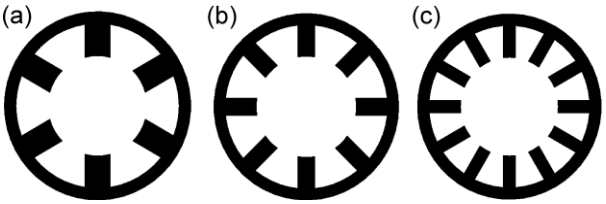

Fig. 3. The XY view of the SRM stators with: (a) N_s = 6, (b) N_s = 8, and (c) N_s = 12.

The XY view of the SRM stators geometry with Ns = 6, 8 and 12 is given in Fig. 3 (a), Fig. 3 (b) and Fig. 3 (c), respectively.

Table 1: Dimensions of the analyzed SRM stators

N_s	6	8	12
w_{sp}	25.82 mm	15.64 mm	13.05 mm
ß	30°	18°	15°
R_{so}	95 mm		
R_{sy}	82.5 mm		
L	114 mm		
w_{sy}	12.5 mm		
R_{si}	50 mm		
h_p	32 mm		

The width of the stator pole and the stator pole arc were adjusted to each of the stator geometry according to the design recommendations for the SRM stator sizing [15]. The stator was modeled as a solid/bulk material without taking into account the laminations. The used material for the stator yoke is M270-35A. The dimensions of the SRM stators geometries analyzed in this study are listed in Table 1.

Within this part of the study, the influence of modification of the stator yoke thickness w_{sy} and the height of the stator poles (i.e., stator teeth) h_p on the stator natural frequencies was numerically investigated. The parameterization of the SRM stator geometry was carried out by modifying the stator yoke thickness and height of the stator pole with respect to the dimension

of the baseline model dimensions w_{sy} = 12.5 mm and h_p = 32 mm by increments of 0.5 mm. In this way the functional dependency of the studied SRM natural frequencies f [Hz] on yoke thickness f(w_{sy}) and pole height f(h_p) was obtained, as shown in Fig. 4. The numerical simulations show that the increase in height of the stator's pole h_p results in decrease of natural frequency for all studied SRM stator configurations as shown in Fig. 4 (a) and Fig. 4 (b). On the other hand, the Figs. 4 (a) and 4 (b) show that higher number of stator poles (i.e., 6/4 vs. 8/6) yields higher natural frequency of the SRM stator configuration. As for the parameterization of the stator yoke thickness, the SRM stator natural frequencies increased with the increase of the stator yoke thickness Fig. 4 (c) and Fig. 4 (d). This is in agreement with previous findings which demonstrated that undesirable vibrations of the SRM machines can be reduced by employing relatively thick stator yokes to minimize deflection, which in turn increases the mechanical stiffness of the machine [17].

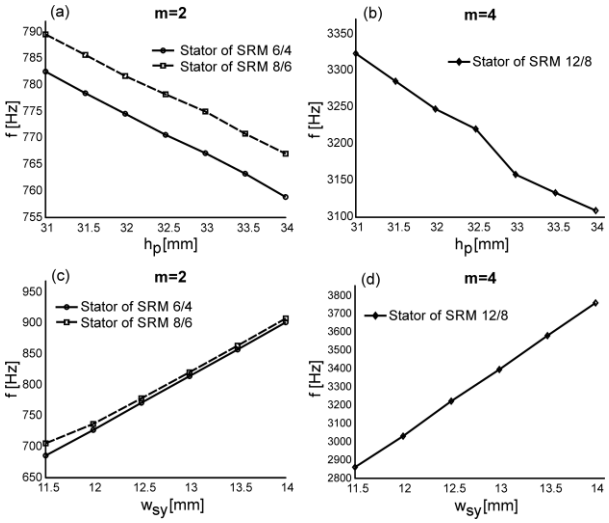

Fig. 4. The calculated relationships: (a) f(h_p) and (b) f(w_{sy}) for the SRM designs with N_s = 6 and N_s = 8, and (c) f(h_p) and (d) f(w_{sy}) for the SRM design with N_s = 12.

Furthermore, the increase of natural frequencies of SRM configuration by adding the aluminum spacers between the stator poles and the end-bells is also numerically calculated. The geometry and placement of the spacers and the end bells added to the reference/ baseline SRM geometries (from Fig. 3) are shown in Fig. 5 (a) and Fig. 5 (b), respectively.

The number of stator poles in SRM designs depends on the number of the excitation voltage phases used (i.e., three phases are needed for the 6/4 SRM design, four phases are needed for the 8/6 SRM; the 6/4 design is two times repeated in the 12/8 design) [15]. The thickness of the spacers inserted between the stator poles depends on the available space within the stators' slots (as well as on the properties of the windings, fill factor, current density and B(H) characteristic of the stator material). In this study the width of the spacers is 5 mm, while the width of the end-bell is 10 mm, Fig. 5. The number of spacers is equal to number of stator poles. Since the end-bells represent the bearing housing, their dimensions thus need to be calculated according to the bearing dimensions. When calculating the end-bell dimensions it is also important to achieve a high enough mechanical strength of the SRM housing in order to efficiently support the mechanical loadings of the shaft. In order to precisely calculate the natural frequencies a 3D numerical modeling need to be used by taking into account the material and geometrical properties of the SRM stator structure.

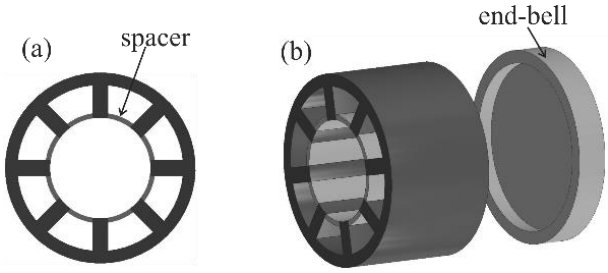

Fig. 5. Geometry and placement of: (a) the spacers between poles, and (b) the spacers between poles and the end-bell added to the baseline geometry of the SRM stators. The width of the spacers is 5 mm. The width of the end-bell is 10 mm.

The results of 3D numerical calculations of stator motion profiles in ZX cross section plane at circumferential mode shapes m = 2 (for SRMs 6/4 and 8/6) and m = 4 (for SRM 12/8) and the corresponding natural frequencies are shown in Fig. 6. The results are displayed in increasing order of the calculated natural frequencies. The calculated natural frequencies and the deflection profiles of the baseline SRM stators with N_s = 6, N_s = 8 and N_s = 12 are shown Figs. 6 (a), 6 (b) and 6 (c). The numerical results show the natural frequencies can be increased by adding the end-bells to the stators as shown in Figs. 6 (d), 6 (e) and 6 (f).

The natural frequencies can be further increased by adding the spacers between the stator poles (Figs. 6 (g), 6 (h) and 6 (i)). The integration of the spacers and end-bell together yields the highest increase in natural frequencies as shown in Figs. 6 (j), 6 (k) and 6 (l). The increase in natural frequencies of the stators due to different stator modifications with respect to the natural frequencies of the reference stator models with N_s = 6, N_s = 8 and N_s = 12 is evaluated and compared in Table 2. The natural frequency (f) of the modified stators is divided by the natural frequency of the reference stator model (f_0) (i.e., factor f/f_0 in Table 2). The factor f/f_0 is

calculated for the stators with one end-bell (no spacers), with spacers (and no end-end-bells), with one end-bell and spacers, two end-bells (and no spacers) and with two end-bells and spacers. As shown in Table 2, the integration of two end-bells and spacers yields the highest increase in natural frequencies (i.e., by factors 3.97, 4.15 and 2.44).

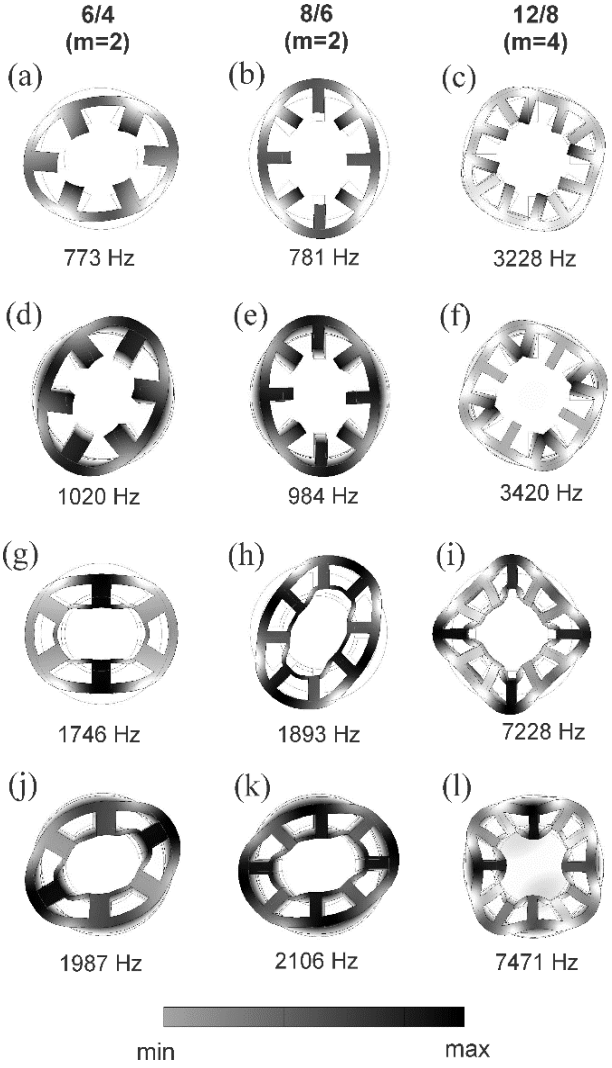

Fig. 6. Comparison of 3D numerical modeling results for the SRM stators with N_s = 6, 8 and 12.

In conclusion, the results of 3D numerical modeling (Fig. 6 and Table 3) demonstrate that the stator modifications such as integration of spacers and/or end-bells constraint the intensity of the stators' motion and significantly increase the natural frequencies of the SRM stators. This may in turn result in reduction of undesirable noise and vibration that may be produced by the SRM.

Table 2: Natural frequencies of the modified SRM stator models (f) with respect to the natural frequencies of the reference/baseline SRM stator models (f_0) with N_s = 6, 8 and 12

SRM 6/4		SRM 8/6		SRM 12/8	
m = 2		m = 2		m = 4	
(Hz)	f/f_0	(Hz)	f/f_0	(Hz)	f/f_0
Reference Stator (f_0):					
773	1	781	1	3228	1
With One End-bell (f):					
1020	1.32	984	1.26	3420	1.06
With Spacers (f):					
1746	2.26	1893	2.42	7228	2.24
With One End-bell and Spacers (f):					
1987	2.58	2106	2.70	7472	2.31
With Two End-bells (f)					
2496	3.23	2595	3.32	7785	2.41
With Two End-bells and Spacers (f):					
3068	3.97	3241	4.15	7878	2.44

C. Influence of stator pole geometry modifications on natural frequencies

Within the third part of the study, the influence of modification of stator pole geometry (i.e., stator teeth) on the natural frequencies of the SRM stator was numerically investigated. The stator geometry modifications were done on the SRM stator with N_s = 12. Three different modifications of the reference/baseline stator pole geometry (shown in Fig. 7 (a)) were done as follows: the first modification of the baseline stator pole was a trapezoidal pole (Fig. 7 (b)), the second one was trapezoidal pole with a circumference (Fig. 7 (c)) and the third one was a trapezoidal pole with a circumference of pole and the pole's root (Fig. 7 (d)). The geometrical modifications with respect to the reference/baseline geometry are marked with red color in Fig. 7. The results of numerical modeling are displayed in order of increasing natural frequency for different studied geometries in Fig. 8.

The numerical results in Fig. 8 show that the natural frequencies of the stator can be altered by modifying the stator pole geometry. The highest natural frequency as compared to the reference/baseline model (shown in Fig. 8 (a)) is obtained with the trapezoidal pole with a circumference of pole and pole's root as shown in Fig. 8 (d) (i.e., from 3228 Hz to 3593 Hz). These results can be particularly useful for the SRM designs which require higher input currents and thus more space for the windings with a larger cross section area of the wire. Similar increase in natural frequency by modifying the stator pole geometry can be obtained in other SRM configurations (e.g., 6/4 and 8/6 SRM stator designs). However, the geometrical modifications of the poles

need to be selected according to the desired winding fill factor and the stator magnetic load ability.

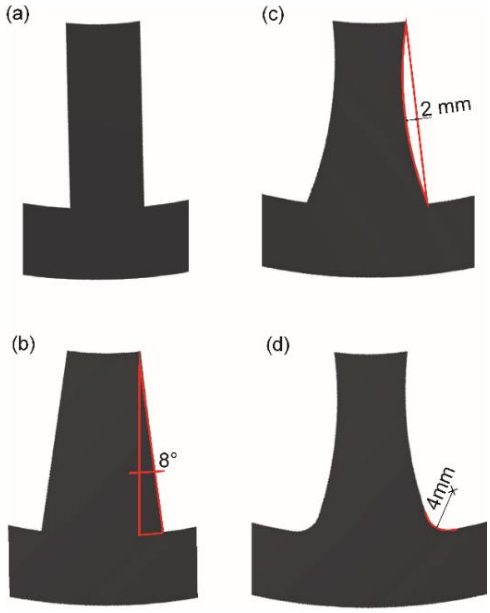

Fig. 7. The reference/baseline stator pole geometry the SRM 12/8 (a) and the modified stator poles (b) trapezoidal pole; (c) trapezoidal pole with a circumference, and (d) trapezoidal pole with a circumference of pole and the pole's root.

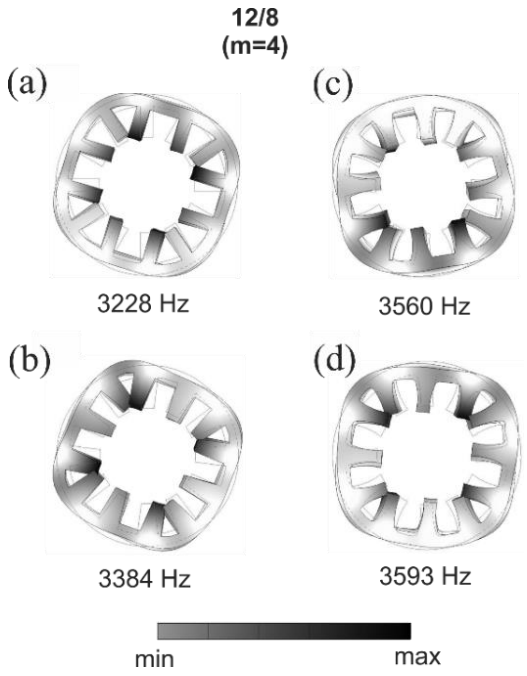

Fig. 8. Numerical results: (a) the reference/baseline stator pole geometry, (b) trapezoidal pole, (c) trapezoidal pole with a circumference, and (d) trapezoidal pole with a circumference of pole and pole's root.

D. Comparison between numerical and analytical results

Within the final part of the study the natural frequencies of the studied baseline SRM stator geometries were also analytically calculated by employing Jordan's law (Equations (2), (3) and (4)). The analytical results (i.e., calculated natural frequencies of the stators approximated with cylindrical rings in 2D) are compared to the numerically calculated natural frequencies of the SRM stators in 3D (Table 3).

Table 3: Comparison between numerical and analytical results

N_s and m	Analyt. (Hz)	Numer. (Hz)	Difference (%)
$N_s = 0$, $m = 2$	962	982	2
$N_s = 0$, $m = 4$	5218	5174	0.85
$N_s = 6$, $m = 2$	736	773	5
$N_s = 8$, $m = 2$	768	781	1.8
$N_s = 12$, $m = 4$	3991	3228	23

The smallest difference is obtained between the numerical model of hollow cylinder (stator without poles $N_s = 0$) and the analytical solution (with the corrective factor $\Delta_m = 0$) (i.e., 2% and 0.85% for $m = 2$ and $m = 4$, respectively). However, this model can result in erroneous calculations of natural frequencies if used as an approximation for the SRM stators with teeth/poles (e.g., f = 733 Hz for the SRM ($N_s = 6$, $m = 2$) vs. f = 962 Hz for the SRM ($N_s = 0$, $m = 2$), Table 3).

As for the stator models with poles, better agreement was obtained between numerical and analytical results for the modal shapes $m = 2$ (the difference between the numerical and analytical results was 5% and 1.8%, for 6/4 and 8/6 SRM, respectively) as compared to the results calculated for modal shapes $m = 4$ for 12/8 SRM stators (the difference between the numerical and analytical results was 23%). The comparison between the analytical and numerical results (Table 3) implies that analytical solution obtained by using Jordan's law (if the corrective factor is taken into account) is good enough to be used as a rapid, but rough estimation of natural frequencies of the SRM stators for modal shapes $m = 2$. A precise calculation of natural frequencies requires a detailed 3D numerical modeling by considering all geometrical and material properties.

The difference between the analytical and numerical results occurs due to the fact that the analytical results are obtained using Jordan's law which describes the natural frequency of a cylindrical ring which approximates the geometry of the SRM with multiple poles in 2D, while the numerical calculation are performed for the SRM stator geometry in 3D [14]. Better agreement between the two sets of results can be obtained by considering solutions of extended Jordan's law [14], or more complex analytical models [12,14].

IV. CONCLUSION

The natural frequencies and thus the level of acoustic noise and vibration strongly depend on geometrical properties of the SRM stator which need to be carefully planned and designed within the pre-construction stage. This study proposes the solutions on how to select an appropriate stator SRM geometry in order to increase its natural frequencies beyond the operational frequencies, and thus to mitigate the electromagnetically excited noise and vibration of the SRM. The natural frequencies of different SRM stator configurations were numerically and analytically investigated by virtue of modal analysis theory. The obtained results are successfully verified based on the previously published theoretical and experimental data.

The obtained results demonstrate that the natural frequencies of the SRM stator can be increased, and thus the noise and vibration can be mitigated by performing the following stator modifications: 1) by increasing the number of the stator pole, 2) by decreasing the height of the stator pole, 3) by increasing the thickness of the stator yoke, 4) by inserting the spacers between the poles, 5) by adding the end-bells, and 6) by modification of the stator pole geometry. On the other hand, the numerical simulations show that the increase in height of the stator's poles results in decrease of natural frequency.

Based on the comparison between the numerical and analytical results it can be concluded that that analytical solution by using Jordan's law is good enough to be used as a rapid first estimation of natural frequencies for the modal shape $m = 2$. However, for precise calculation of natural frequencies the detailed 3D numerical analysis considering all geometrical and material properties of SRM need to be used.

The results obtained in this study can provide useful guidelines for further experimental testing and design of SRM machines as well as for other types of electrical machines. Namely, the results can be successfully used in further investigations on the undesirable noise and vibration emitted from the SRM which could also consider the whole stator assembly comprising the windings, the insulation components as well as the stator laminations needed for axial modal shape analysis. In addition, further investigation of adequate SRM configurations can also involve different optimization procedures; the results obtained in this study can therefore be successfully used as input data into the optimization algorithms. To conclude, the findings provided in this study can have important implication in efficient machine design planning and manufacturing process of a SRM with significantly reduced magnetically excited noise and vibration.

ACKNOWLEDGEMENT

This study was conducted within the project entitled Premium Efficiency Class Electrical Motors with ID L2-8187 (C). The authors acknowledge the project (Premium Efficiency Class Electrical Motors, ID L2-8187 (C)) was financially supported by the Slovenian Research Agency.

REFERENCES

[1] M. Yilmaz, "Limitations/capabilities of electric machine technologies and modeling approaches for electric motor design and analysis in plug-in electric vehicle applications," *Renew Sust. Energ. Rev.*, vol. 52, pp. 80-99, 2015.

[2] M. Takiguchi, H. Sugimoto, N. Kurihara, and C. Chiba, "Acoustic noise and vibration reduction of SRM by elimination of third harmonic component in sum of radial forces," *IEEE Trans. Energy Convers*., vol. 30, pp. 883-891, 2015.

[3] T. J. E. Miller, "Optimal design of switched reluctance motors," *IEEE T. Ind. Electron*., vol. 49, pp. 15-27, 2002.

[4] R. Krishnan, D. Blanding, A. Bhanot, A. M. Staley, and N. S. Lobo, "High reliability SRM drive system for aerospace applications," In: *The 29th Annual Conference of the IEEE Industrial Electronics Society (IECON 2003)*, Roanoke, VA, USA: IEEE, pp. 1110-1115, 2-6 Nov. 2003.

[5] S. Haghbin, A. Rabiei, and E. Grunditz, "Switched reluctance motor in electric or hybrid vehicle applications: A status review," In: *The 8th IEEE Conference on Industrial Electronics and Applications (ICIEA 2013)*, Melbourne, Australia: IEEE, pp. 1017-1022, 19-21 June 2013.

[6] Z. Xu, D. H. Lee, and J. W. Ahn, "Design and operation characteristics of a novel switched reluctance motor with a segmental rotor," *IEEE T. Ind. Appl*., vol. 52, pp. 2564-2572, 2016.

[7] S. Song, S. Chen, and W. Liu, "Analytical rotor position estimation for SRM based on scaling of reluctance characteristics from torque-balanced measurement," *IEEE T. Ind. Electron*., vol. 64, pp. 3524-3536, 2017.

[8] W. Wang, M. Luo, E. Cosoroaba, B. Fahimi, and M. Kiani, "Rotor shape investigation and optimization of double stator switched reluctance machine," *IEEE T. Mag.*, vol. 51, pp. 8103304, 2015.

[9] W. Cai, P. Pillay, and Z. Tang, "Impact of stator windings and end-bells on resonant frequencies and mode shapes of switched reluctance motors," *IEEE T. Ind. Appl.*, vol. 38, pp. 1027-1036, 2002.

[10] P. C. Desai, M. Krishnamurthy, N. Schofield, and A. Emadi, "Novel switched reluctance machine configuration with higher number of rotor poles than stator poles: Concept to implementation," *IEEE T. Ind. Appl.*, vol. 57, pp. 649-659, 2010.

[11] C. Lin and B. Fahimi, "Prediction of acoustic noise in switched reluctance motor drives," *IEEE T. Energy Conver.*, vol. 29, pp. 250-258, 2014.

[12] M. N. Anwar and I. Husain, "Radial force

calculation and acoustic noise prediction in switched reluctance machines," *IEEE T. Ind. Appl.*, vol. 36, pp. 1589-1597, 2000.
[13] T. Lachman, T. R. Mohamad, and G. L. A. Onyango, "Analytical methods for prediction of acoustic noise generation in switched reluctance motors," In: *IEEE International Conference on Robotics, Intelligent Systems and Signal Processing*, Changsha, Hunan, China: IEEE, pp. 226-231, 8-13 Oct. 2003.
[14] J. P. Lecointe, R. Romary, J. F. Brudny, and T. Czapla, "Five methods of stator natural frequency determination: Case of induction and switched reluctance machines," *Mech. Syst. Signal Pr.*, vol. 18, pp. 1133-1159, 2004.
[15] R. Krishnan, *Switched Reluctance Motor Drives: Modeling, Simulation, Analysis, Design, and Applications*. Boca Raton, FL, USA: CRC Press, 2001.
[16] H. Jordan, *Geräuscharme Elektromotoren: Lärmbildung und Lärmbeseitigung bei Elektromotoren*. Essen: Girardet, 1950.
[17] S. A. Long, Z. Q. Zhu, and D. Howe, "Vibration behavior of stators of switched reluctance machines," *IET Electr. Power App.*, vol. 148(3), pp. 257-264, 2001.
[18] B. T. Wang and D. K. Cheng, "Modal analysis of mdof system by using free vibration response data only," *Journal of Sound and Vibration*, vol. 311, pp. 737-755, 2008.

Selma Čorović received her Ph.D. degrees from the Faculty of Electrical Engineering, University of Ljubljana and from the University of Paris XI, France. She is as an Assistant Professor with the Department of Mechatronics, Faculty of Electrical Engineering at the University of Ljubljana. Her research interests include coupled analysis, modeling and optimization of electrical machines (generators, motors, transformers and actuators) and electromagnetics and mechanics in biomedical engineering.

Rok Benedetič received the B.Sc. degree in Electrical Engineering from University of Ljubljana, Slovenia, in 2016. His research interests include analysis and modeling of electrical machines.

Damijan Miljavec is a Full Professor with the Department of Mechatronics and is the Head of Laboratory for Electrical Machines, Faculty of Electrical Engineering, University of Ljubljana. His research interests include analysis, modeling, design and optimization of conventional and unconventional electric machines, design of actuators, introduction of new materials, EMC characteristics of electric machines and coupled analysis in electrical machines. He has co-authored several papers published in SCI indexed scientific journals, several papers in conference proceedings and one international patent.